LA-NUREG-6377-MS
Informal Report

NRC-8

c. 3

Seismic Response of a Block-Type Nuclear Reactor Core

Issued: July 1976

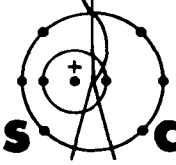

los alamos
scientific laboratory
of the University of California
LOS ALAMOS, NEW MEXICO 87545

UNITED STATES
ENERGY RESEARCH AND DEVELOPMENT ADMINISTRATION
CONTRACT W-7405-ENG. 36

This work was supported by the US Nuclear Regulatory Commission, Division of Reactor Safety Research.

Printed in the United States of America. Available from
National Technical Information Service
U.S. Department of Commerce
5285 Port Royal Road
Springfield, VA 22161
Price: Printed Copy $3.50 Microfiche $2.25

LA-NUREG-6377-MS
Informal Report
NRC-8

los alamos
scientific laboratory
of the University of California
LOS ALAMOS, NEW MEXICO 87545

Seismic Response of a Block-Type Nuclear Reactor Core

by

Richard C. Dove
Joel G. Bennett
Jean L. Merson

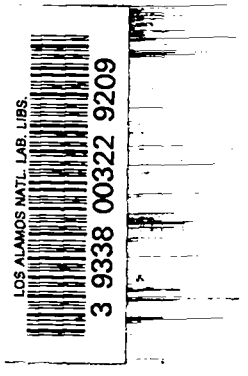

Manuscript completed: May 1976
Issued: July 1976

Prepared for the US Nuclear Regulatory Commission
Office of Nuclear Regulatory Research
Contract W-7405-ENG.36

SEISMIC RESPONSE OF A BLOCK-TYPE NUCLEAR REACTOR CORE

by

Richard C. Dove, Joel G. Bennett, and Jean L. Merson

ABSTRACT

An analytical model is developed to predict seismic response of large gas-cooled reactor cores. The model is used to investigate scaling laws involved in the design of physical models of such cores, and to make parameter studies.

I. INTRODUCTION

The use of a large number of graphite elements to form the core of a nuclear reactor is not new. However, a recent core design for a large gas-cooled reactor contains a very large number of graphite blocks, and in accord with present practice the seismic response of this core must be accurately predicted. Such a system of blocks does not constitute a structure in the usual sense, and hence the theory and experimental data available for the prediction of seismic response cannot be directly applied. This paper describes an analytical model that has been developed to predict the response of a system of blocks (representative of a simplified reactor core) to general seismic input. This model was then used to investigate scaling laws developed as part of a program to physically scale reactor cores of this type. A parameter study was made to determine the relative importance of material properties, design features, and test conditions associated with a given core design.

II. THE PHYSICAL SYSTEM

Nuclear reactor cores that consist of graphite blocks of various shapes have been described by several authors. The physical system of interest in this investigation is one described by Neyland and Gorholt.[1] This core system, for use in large high-temperature gas-cooled reactors (HTGR's), was developed by the General Atomic Company of San Diego, California. The core consists of a large number of hexagonally shaped graphite blocks with a great number of degrees-of-freedom (ultimately, six motion coordinates times "n" blocks, or as many as 23,664 degrees-of-freedom), and with complicated boundary and support conditions.

III. THE ANALYTICAL MODEL

Ideally, the model should consist of a three-dimensional array of elements that can be: 1) extended in number as required, 2) given any shape, 3) connected to each other by any means, 4) assigned any physical property values, 5) supported and restrained on the array's exterior boundaries by any means, 6) excited by three independent axial motions representing three earthquake components, and 7) for which the six components of motion and all forces can be computed for each element. Such a general model is not practical, and the simplified model discussed below incorporates the most important governing characteristics of the real system. The elements are taken as cubic in shape (this is not required as part of the simplification), and are connected to each other by dowels in sockets. They are contained in a surrounding structure, which, although

having a finite stiffness on contact with the core blocks, moves as a unit under the influence of seismic excitation. The model can be driven by independent motion inputs, but rotational response or coupling between rotational response and linear response is not considered. The core blocks can be assigned desired values for physical properties including stiffness (modulus), density, inelastic energy loss, and coefficient of friction between blocks.

Figure 1 is a free-body diagram of a core block showing the forces that are allowed to act upon it. A number of these blocks are then arranged in one- or two-dimensional arrays and subjected to one or two independent motion-time inputs. Figure 2 illustrates a two-dimensional array.

The significant difference between this model and the usual structural model is that it uses Coulomb friction rather than viscously damped spring-masses. The analytical method uses the component element method combined with an equilibrium iteration procedure.

Figure 3 illustrates a flow chart of the equilibrium iteration scheme used. The philosophy is to trace the time history of each block through a succession of equilibrium states, each new state being based on the previous configuration.

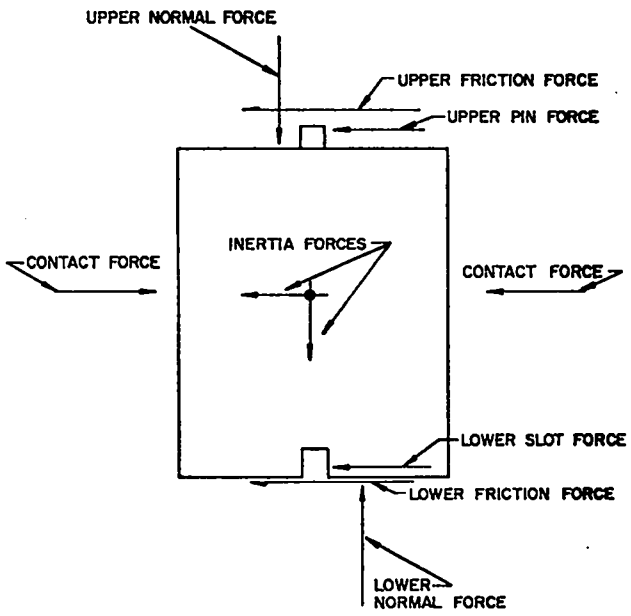

Fig. 1. Forces acting on core block.

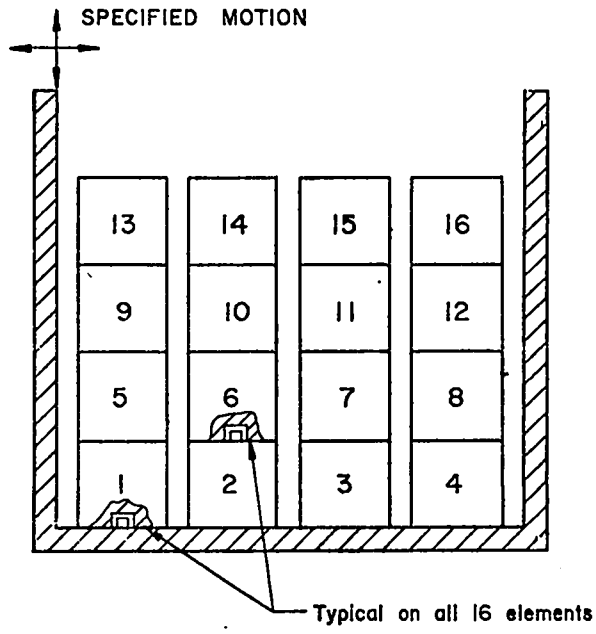

Fig. 2. Two-dimensional model.

The first step for this procedure is to determine the initial acceleration of each block from equilibrium considerations ($\Sigma F = Ma$). This step assumes that the temporal history of the boundary displacement is known. The initial forces are determined from force-displacement curves.

The accelerations from this step are extended forward in time by predicting the acceleration that will exist at the end of a small time increment. This predicted acceleration is then integrated twice using a time integration scheme such as the Newmark β, or Wilson θ, or other methods. The current program makes use of the Newmark method with $\beta = 0.25$ for which the expressions for velocity and displacement are simple finite difference expressions of the truncated Adams type.[2] Using these displacements, the corresponding forces on all blocks must be determined from known force-displacement information.

The model can accommodate inelastic energy loss during impact. Figure 4 illustrates a typical loading and unloading path during the impact sequence, where the area enclosed represents energy lost. The advantage of this model is that the energy lost can be specified as a percentage of the energy stored during the loading sequence. In practice this is done by specifying the percentage energy loss, which defines the unloading modulus D through

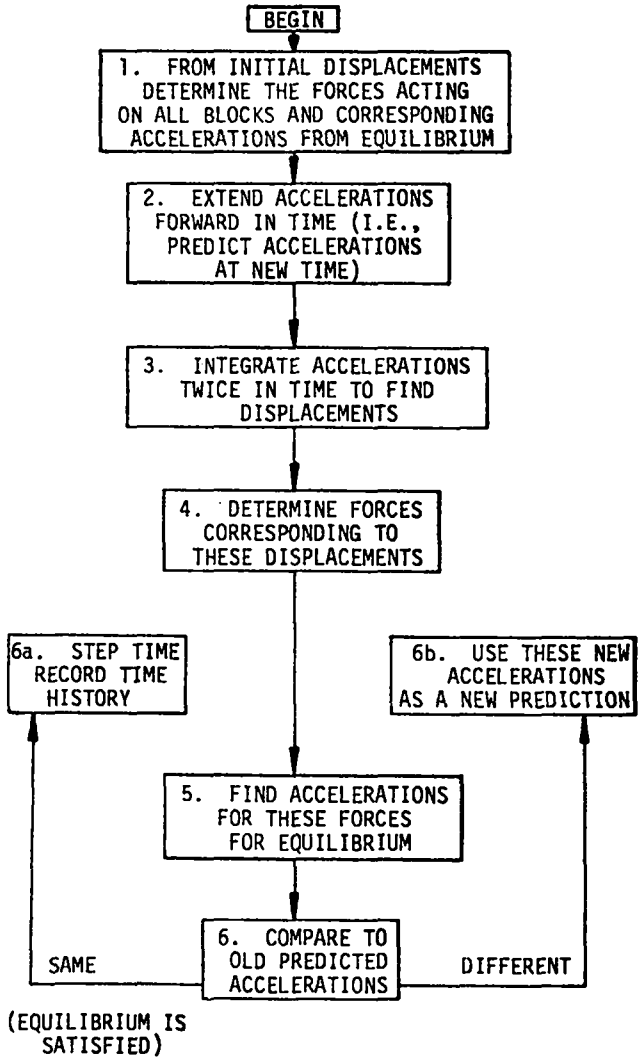

Fig. 3. Equilibrium iteration scheme.

the relationship.

$$D = E - \frac{\%\ \text{Energy Loss}}{100} E.$$

The disadvantage of this model is that it does not take into account the accumulating permanent deformation. It should be recognized that this method can be used equally well for nonlinear force-displacement elements. However, the more sophisticated the force-displacement information, the more costly the time-history analysis will be.

All forces determined from computed displacements are now applied to the blocks and their

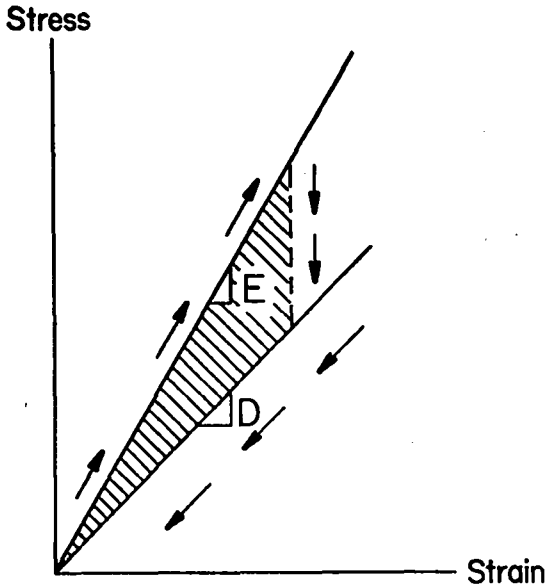

Fig. 4. Inelastic energy loss model.

corresponding accelerations determined from equilibrium considerations. These new accelerations are compared to the values predicted, and if they agree within a given tolerance, a dynamic equilibrium state has been attained. In this case, time is incremented and the equilibrium state is recorded as the time history of the system.

For the case where agreement with predicted values is not obtained, the accelerations found by applying the force-displacement information are used as a new prediction, and the integration step is repeated. This iteration process is continued until agreement is obtained.

The program[3] used for the solution of the equations of motion has the following characteristics:

a. The input motions to the axes are independent.

b. The input motions may be in the form of analytic functions (sinusoidal, etc.), or externally generated motion-time records (simulated or real earthquake time histories).

c. Computer generated movies can be used to display position versus time information.

d. For each block in the system the displacement time-, acceleration time-, and the force time-histories are available.

IV. DEVELOPMENT OF THE SCALING LAWS

Because the reactor cores are large and massive,

it is necessary to perform seismic testing on scale models. For this reason the appropriate scaling laws for the block-type core under consideration have been developed. For the systems shown in Fig. 2 we may write:

$$X = \phi\ (X_B,\ t,\ d,\ c,\ \rho,\ Q,\ E_{1,2\cdots n},\ D_{1,2\cdots n},\ \sigma_{1,2\cdots n},\ g),$$

where the terms are defined as follows.

- X = response motion of any point, a function of time (t)
- X_B = input motion, a function of time (t)
- t = time
- d = block dimension
- c = clearance
- ρ = block material density
- Q = any external force applied to a block (including friction)
- $E_{1,2\cdots n}$ = moduli of elasticity of the block
- $D_{1,2\cdots n}$ = unloading moduli
- $\sigma_{1,2\cdots n}$ = stress levels used to define the stress versus strain characteristics of the block material
- g = gravitational constant

As many values as are necessary to define the shape of the stress-strain curve may be assigned for E, D, and σ. Inelastic energy loss is accommodated by allowing the unloading curve to differ from the loading curve.

The input (X_B) could be in terms of velocity ($\dot{X}_B$) or acceleration ($\ddot{X}_B$) without affecting the analysis that follows; likewise, the response (X) of the system could be in terms of velocity, acceleration, or block contact forces. These 14 terms can be arranged into 11 dimensionless groups that give

$$\frac{X}{d} = \psi\ \left(\frac{c}{d},\ \frac{X_B}{d},\ \frac{\rho d^2}{t^2 E},\ \frac{E_1 d^2}{Q},\ \frac{gt^2}{d},\ \frac{E_n}{E_1},\ \frac{\sigma_n}{E_1},\ \frac{\sigma_n}{\sigma_1},\ \frac{D_n}{E_1},\ \frac{D_n}{D_1}\right)$$

as the governing equation for this system.*

*See Ref. 4 for a general discussion of dimensional analysis and similitude theory.

From this governing equation we can determine the scale factors necessary to design a model, and relate model response to prototype response. Having selected the materials for both the model and the prototype, two scales are fixed. First, the density scale N_ρ is given by

$$N_\rho = \frac{\rho_p}{\rho_m},$$

where

- ρ_p = prototype density, and
- ρ_m = model density.

Likewise, the modulus scale is

$$N_E = \frac{E_p}{E_m},$$

where

- E_p = prototype modulus, and
- E_m = model modulus.

Equation 2 requires that

(a) the length scale ($N_d = \frac{d_p}{d_m}$) be $N_d = \frac{N_E}{N_\rho}$,

(b) the time scale ($N_t = \frac{t_p}{t_m}$) be $N_t = \sqrt{N_d}$, and

(c) the force scale ($N_Q = \frac{Q_p}{Q_m}$) be $N_Q = N_E N_d^2$.

In addition, the five terms ($\frac{E_n}{E_1}$, $\frac{\sigma_n}{E_1}$, $\frac{\sigma_n}{\sigma_1}$, $\frac{D_n}{E_1}$, and $\frac{D_n}{D_1}$) indicate that the material used for the model must have stress-strain characteristics similar to the prototype material.

These scales and design conditions are very restrictive. For example, the simplest way to insure that model and prototype materials have the required similarity is to use the same material for both. However, this gives a value of unity for both density scale and modulus scale ($N_\rho = 1$, $N_E = 1$) that in turn dictates that the length scale be unity. Hence, a scale model is not possible unless some way is found to adjust the mass independent of material density.

If a different material is used for the model it must have a smaller modulus (E) to density (ρ) ratio than the prototype material (graphite, in the case of a reactor core). At first glance, this does not seem to be a difficult condition to fulfill,

and indeed a number of plastics have ratios of E to ρ that result in models of between 1/5 and 1/10 the size of the graphite prototype. However, if stresses in either the model or the prototype exceed values beyond which the material behavior can be described in terms of a single modulus value (E_1), there is no assurance (without further analysis) that the model and prototype will exhibit the required similarity.

If the gravitational constant (g) is omitted from the governing variables in Eq. (1), the term ($\frac{gt^2}{d}$) does not appear in Eq. (2). For this case the length scale ($N_d = \frac{d_p}{d_m}$) can be selected as any desired value, since it is independent of the density scale (N_ρ) and the modulus scale (N_E). For this case (g, omitted) where the same material is used for the model and prototype, the time scale (N_t) is equal to the length scale (N_d). The question is: Does the behavior of the system depend upon "g"? The force of gravity does affect this system if frictional forces are important, since frictional forces are proportional to normal forces which are dependent on the block weight (hence, "g"), and any vertical acceleration. To omit "g" is to distort all frictional effects, and these may be the major damping mechanism.

V. USE OF THE ANALYTICAL MODEL

The analytical model described has been used to investigate the scaling laws developed above and to conduct a parameter study. The purpose of these investigations has been to prepare for physical model testing.

In order to investigate the scaling laws the one-dimensional system shown in Fig. 5 was considered. Four different systems having the parameters shown in Table I were run. All three of the "models" are designed with a length scale (N_d) of 4, but differ greatly in other ways. The "true model" is designed to satisfy all of the scale relationships dictated by the laws of similitude.

Figure 6 shows the acceleration response of block #1 in the prototype system to a ± 1g, 5-Hz excitation. Figure 7 shows the acceleration response of block #1 in the true model system to a ± 1g, 10-Hz excitation (since model times are scaled by dividing by 2, i.e., N_d, frequencies are doubled). Inspection of these two acceleration time-histories shows that when properly scaled ($N_{\ddot{X}} = 1$, $N_t = 2$), the true model predicts the prototype acceleration time-history. The prediction is most accurate during early times, and as time progresses, cumulative computational errors produce some divergence of results.

The next system considered is referred to in Table I as a "distorted model." This model is distorted in the following way: having picked a length scale (N_d) arbitrarily, the same material is used for the model as for the prototype. As a result, the material modulus of the model equals the material modulus of the prototype ($E_m = E_p$). Since, for equal material density, weight varies as the

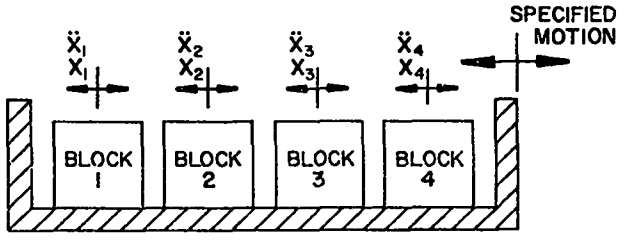

Fig. 5. One-dimensional model.

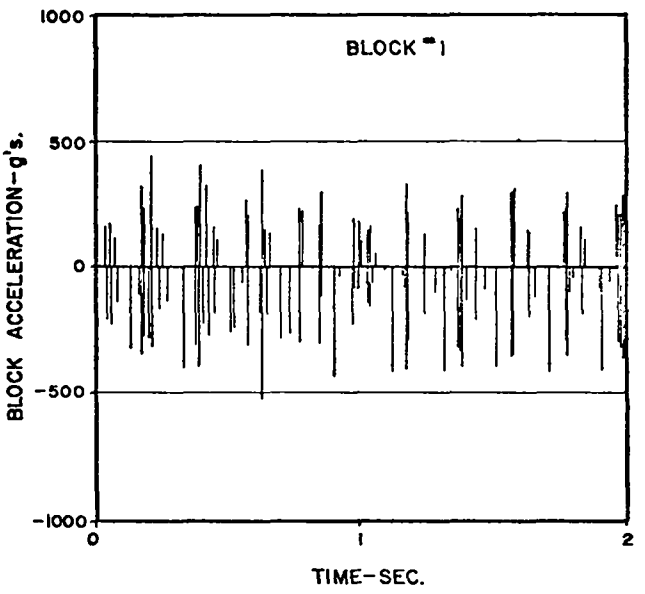

Fig. 6. Prototype response.

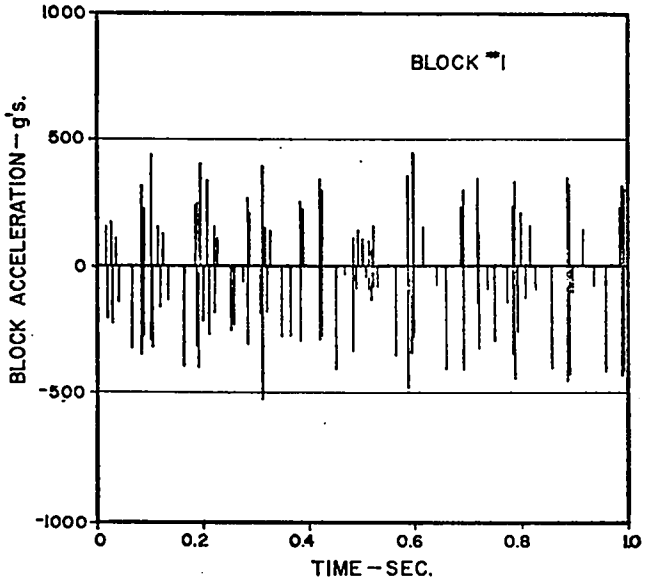

Fig. 7. True model response.

cube of the dimension, then $W_m = W_p/N_d^3$. The result is a model that is too light for its stiffness if tested in the same gravitational field as the prototype. These choices also result in a time scale equal to the length scale ($N_t = N_d$) and an acceleration scale equal to the reciprocal of the length scale ($N_{\ddot{X}} = 1/N_d$). Figure 8 shows the acceleration response of block #1 in this distorted model system to a $\pm$ 4g, 20-Hz excitation (model accelerations are four times prototype accelerations and since model

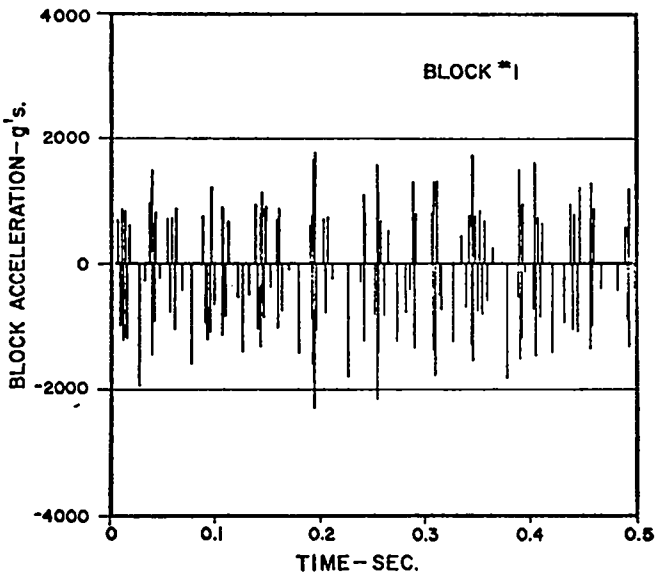

Fig. 8. Distorted model response.

times are scaled by dividing by 4, frequencies are multiplied by 4). Comparison of this record to the prototype system acceleration response (Fig. 6) indicates how this system response differs from the prototype. We note that in the distorted model the impacts are more uniformly spaced in time, and that although the peak accelerations occur at different times, the distorted model predicts (when properly scaled) the peak values with reasonable success. However, study of the displacement versus time-histories shows that this distorted model responds with a completely different displacement time-history from the prototype.

The fourth system considered is referred to as a "friction-corrected distorted model" in Table I. This system results from the observation that since the distorted model is too light, and hence frictional forces are too small in a 1g field, a correction should be possible by increasing the coefficients of friction.* Accordingly, both the static and kinetic coefficients of friction (μ_s and μ_k)have been increased by a factor of four. Figure 9 shows the acceleration response of block #1 in this "corrected" system to a $\pm$ 4g, 20-Hz excitation. Comparison of Fig. 9 to Fig. 6 shows that this corrected model predicts the prototype acceleration response exactly (model results must, of course, be scaled, i.e., $\ddot{X}_p = \ddot{X}_m/4$, $t_p = 4 \times t_m$). This correction also allows the model to accurately predict prototype displacement time-histories. Whether this simple type of correction would be physically possible or completely effective in a three-dimensional model subjected to three orthogonal motion inputs is still unknown.

A parameter study was also conducted using the analytical model applied to the one-dimensional system shown in Fig. 5. This one-dimensional model is characterized by the following functional equation (a less general form of Eq. 1).

$$\ddot{X} = \phi\ (X_B,\ t,\ d,\ c,\ W,\ \mu_s,\ \mu_k,\ E,\ D,\ g) \quad (3)$$

in which

$\ddot{X}$ = acceleration of a block

X_B = amplitude of sinusoidal motion applied to the base

*Alternatively, the model might be tested in an artificial higher "g" field.

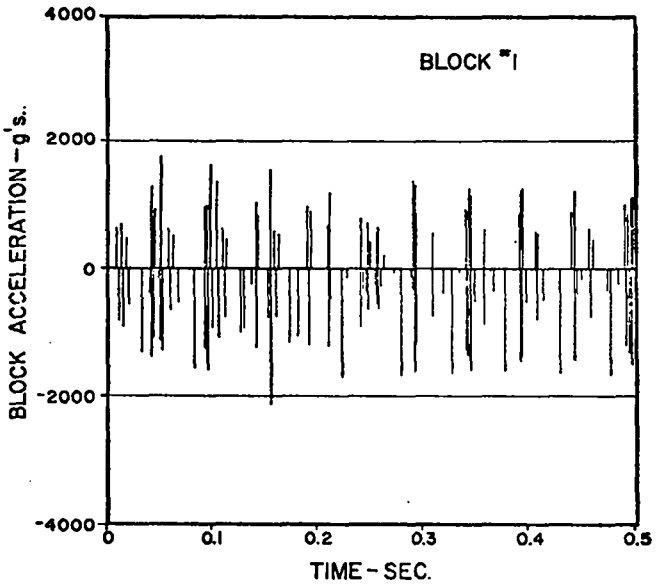

Fig. 9. Friction Corrected Model Response

t = period of input sinusoidal motion or any significant time

d = characteristic block dimension

c = clearance between blocks

W = weight of block

μ_s = static coefficient of friction

μ_k = kinetic coefficient of friction

E = modulus of block, loading

D = modulus of block, unloading

g = gravitational constant.

This functional equation can be rewritten using dimensionless groups as follows:

$$\frac{\ddot{X}}{g} = \Psi \left(\frac{X_B}{d}, \frac{c}{d}, \frac{Ed^2}{W}, \mu_k, \frac{\mu_s}{\mu_k}, \frac{E}{D}, \frac{X_B}{gt^2}\right). \qquad (4)$$

Designating each dimensionless group as a "Pi" term we can write:

$$\pi_1 = \Psi (\pi_2, \pi_3, \pi_4, \pi_5, \pi_6, \pi_7, \pi_8). \qquad (4a)$$

Many other groupings are possible, but this set was chosen to make it easier to vary one "Pi" term while holding the remaining "Pi" terms constant.

In making the parameter study the terms on the right-hand side of Eq. (3) were assigned values, and from these the "base" value of each dimensionless group (π term) on the right-hand side of Eq. (4) was computed. Computer runs were then made in which the value of one π term was varied while all others were held at their base values.

The first investigation was to determine the effect of varying static friction (breakaway friction), μ_s. The data shown on Fig. 10 indicates that variation in μ_s has little effect on the block accelerations.* As a result of this finding, static friction (μ_s) may be eliminated as an independent governing parameter. Figure 11 shows the importance of the clearance gap (c) on block acceleration. It is clear that block acceleration is strongly dependent on clearance. The effect of varying the coefficient of kinetic friction (μ_k) is shown in Fig. 12. The importance of the kinetic friction effect in limiting acceleration is clear.

The effect of energy loss due to inelastic impact was studied by varying π_7, (E/D). The results shown in Fig. 13 indicate that the effect of internal energy loss on block accelerations is relatively small.

From the dimensional analysis (Eq. 4) we see that the effect of block stiffness (E) and block weight (W) can be investigated simultaneously by varying π_4, $(\frac{Ed^2}{W})$. The results of this investigation are shown in Fig. 14.

The purpose of this parameter study was to gain a better physical understanding of the four block one-dimensional model in particular, and block-type nuclear reactor core models in general.

It is also possible to use this parameter study to extend the investigation of the scaling laws. By assuming that the function (ψ) in Eq. (4) is a product form we may rewrite Eq. (4) as

*Provided that the exciting force is large enough to insure that the blocks do break away.

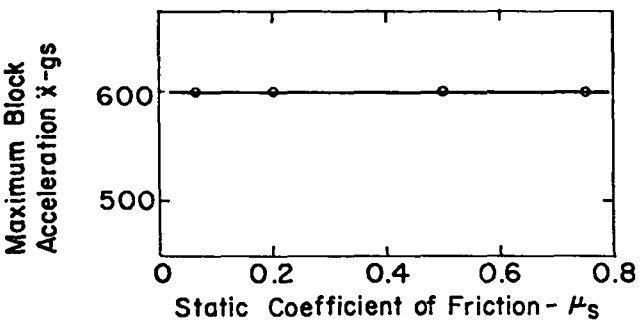

Fig. 10. Effect of static coefficient of friction.

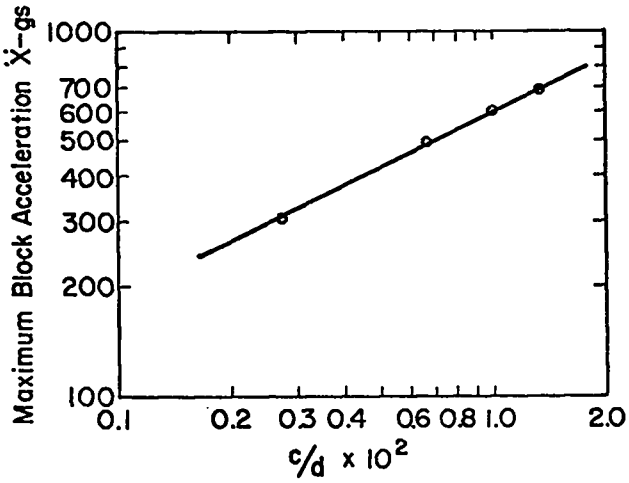

Fig. 11. Effect of block clearance gap.

$$\left(\frac{\ddot{X}}{g}\right) = \psi' \left(\frac{Ed^2}{W}\right) \times \psi'' \left(\frac{X_B}{c}, \frac{c}{d}, \mu_k, \frac{\mu_s}{\mu_k}, \frac{E}{D}, \frac{X_B}{gt^2}\right). \qquad (4b)$$

With a model distorted by using the same material for model and prototype, only the term $\left(\frac{Ed^2}{W}\right)$ need be distorted; so we can write:

$$\frac{\left(\frac{\ddot{X}}{g}\right)_p}{\left(\frac{\ddot{X}}{g}\right)_m} = \frac{\psi'\left(\frac{Ed^2}{W}\right)_p}{\psi'\left(\frac{Ed^2}{W}\right)_m},$$

since the function ψ'' is identical for both model and prototype. The "prediction factor," θ, is

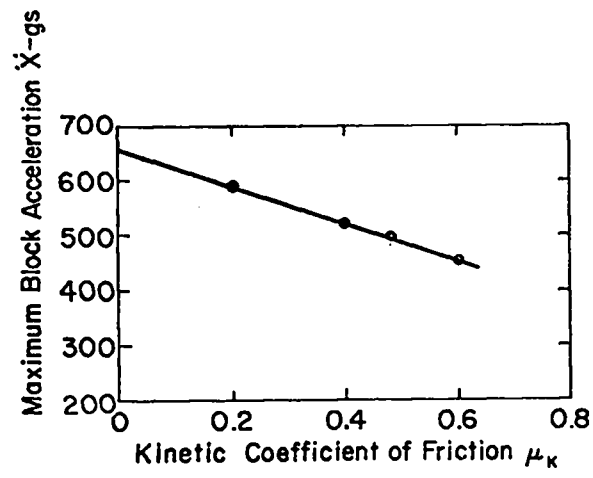

Fig. 12. Effect of kinetic coefficient of friction.

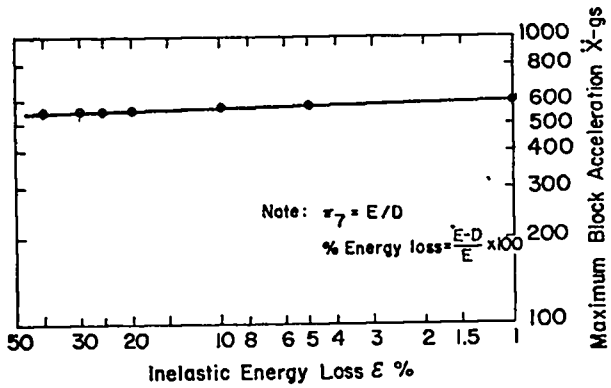

Fig. 13. Effect of inelastic energy loss.

defined as*

$$\theta = \frac{\psi'\left(\frac{Ed^2}{W}\right)_p}{\psi'\left(\frac{Ed^2}{W}\right)_m}, \qquad (5)$$

hence,

$$\left(\frac{\ddot{X}}{g}\right)_p = \theta \left(\frac{\ddot{X}}{g}\right)_m.$$

From the parameter study (Fig. 14) the effect of the term $\frac{Ed^2}{W}$ on block acceleration ($\ddot{X}$) can be expressed as

$$\ddot{X} = 425\sqrt{\left(\frac{Ed^2}{W}\right) \times 10^{-6}}$$

Using this expression for ψ' and substituting in Eq. (5), we can write

$$\theta = \sqrt{\left(\frac{Ed^2}{W}\right)_p \Big/ \left(\frac{Ed^2}{W}\right)_m}.$$

*The procedure for establishing a "prediction factor" that may be used with a distorted model is described in Part II (Distorted Models), Similitude in Engineering, by Glenn Murphy.

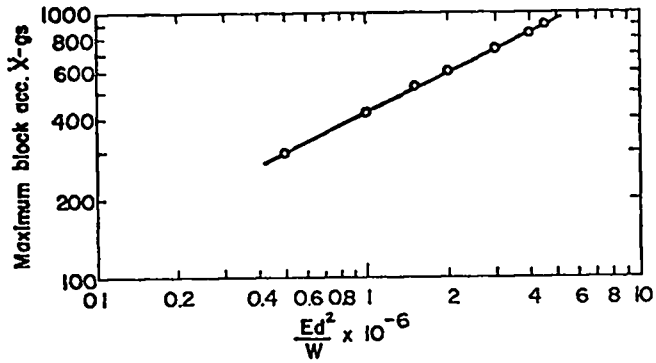

Fig. 14. Effect of modulus to weight ratio.

To test this method of approach, θ was computed from the values of E, d, and W assigned to the "prototype" and "distorted model" systems shown in Table I.

$$\theta = \sqrt{\frac{E_p d^2 p}{W_p}} \Bigg/ \frac{E_p (d_p/N_d)^2}{(W_p/N_d{}^3)}$$

$$\theta = \sqrt{N_d} = \sqrt{4} = 2.$$

The "distorted model" was then tested as if it had been a true model (i.e., $X_B = \pm 0.9944/4cm$, f_B = 10 Hz), and the results multiplied by the prediction factor (θ) to predict prototype response. Figure 15 shows the acceleration response of block #1 in the distorted model system when driven as if it were a true model. Comparison of Fig. 15 with Fig. 6 indicates that when model accelerations are multiplied by a prediction factor (θ) of 2, the prototype acceleration is predicted for homologous times ($t_p = 2\ t_m$). The prediction is most accurate during early times, but as time progresses, cumulative computational errors produce divergence of results.

"Compensated distortion"* is also possible; that is, two or more π terms may be distorted (one or more deliberately in a controlled manner) so as to produce a net prediction factor (θ) of unity. The "coefficient of friction correction of the distorted model" discussed previously is an example of this approach.

Tests in which the exciting force was suddenly reduced to zero indicate that with reasonable values of coefficient of friction, the effective damping is large in this system. Figure 16a-b shows the acceleration-time response for block #1 during two tests. In both cases the system was driven with a ± 1g, 5-Hz, excitation for 0.4 sec (two cycles), after which the excitation was reduced to zero. As shown in Fig. 16b, where the value of the kinetic friction (μ_k) is 0.16, block impacts cease very soon after the excitation goes to zero. This indication of large effective damping indicates that the system has little memory of past acceleration-time history. Therefore, for some purposes the model may be appropriately tested using only selected abbreviated portions of a simulated earthquake time history.*

The analytical model has been applied to the two-dimensional system (Fig. 2) to investigate the effect of the core blocks' pin connections. Values used as "base" data for this model are given in Table II.

Output available for each block (in both tabulated and plotted form) includes: horizontal acceleration, contact force on block side walls, pin force, vertical acceleration, and contact force on block bases, all as functions of time. Figure 17 is an example of a one-second run using base data. Vertical accelerations and forces are not shown,

*Murphy, Similitude in Engineering, pp. 107-108.

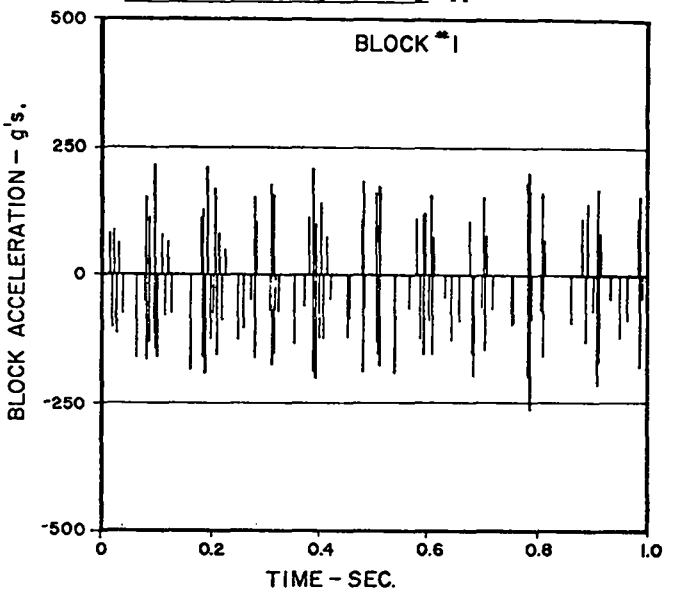

Fig. 15. Distortion factor test.

*An exception to this is when the total number of block collisions is desired (as for a fatigue damage study), rather than maximum values of accelerations or forces.

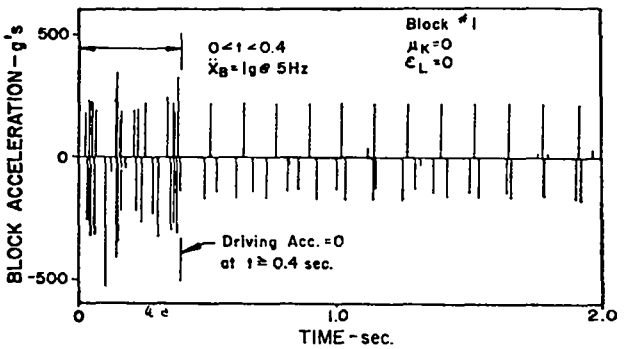

Fig. 16a. Undamped system.

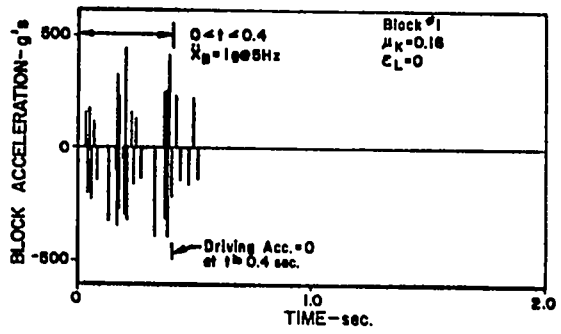

Fig. 16b. Effect of Coulomb damping.

since the vertical input (Y_B) was zero for this case.

The general behavior of the pin-restrained two-dimensional system can be explained in terms of these figures. Although block #9 receives 61 acceleration pulses (Fig. 17a), only two of these are due to side wall impacts (Fig. 17c). The remaining pulses result form pin-slot closure. Those applied to the base of block #9 are shown in Fig. 17b, and those applied to the top of block #9 are available as the equal but opposite reactions for the lower pin forces on block #13.

A series of runs has been made in which pin clearance (h) and pin stiffness (K_p and K_s) have been varied from the base values. The results may be summarized as follows:

a. Side contact between blocks is eliminated in all horizontal rows below which the accumulated pin gap clearance is less than the gap between blocks.

b. Smaller pin/slot clearances (lower "h") produce more numerous, but less intense pin/slot impacts.

c. Stiffer pins (higher values of K_p or K_s) produce more numerous and more intense pin/slot impacts.

Results from several specific runs are summarized in Table III.

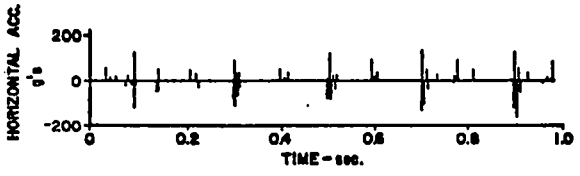

Fig. 17a. Acceleration, block 9; two-dimensional system.

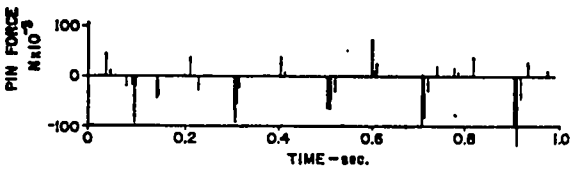

Fig. 17b. Lower pin forces, block 9; two-dimensional system.

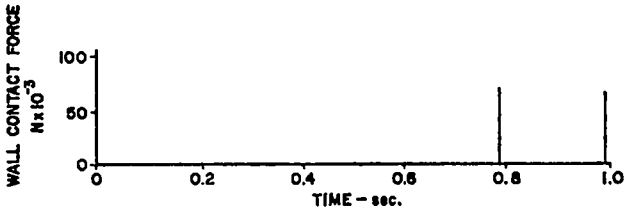

Fig. 17c. Wall contact forces, block 9; two-dimensional system.

VI. CONCLUSIONS

The analytical model described above has been useful in investigating the behavior of this unique system. Clearly the model must be verified, and tests are now being planned that will progressively compare one- and two-dimensional physical systems to the corresponding analytical model. The analytical model is currently being used to determine the effect of vertical acceleration on the response of the two-dimensional system. Simulated earthquake acceleration time-histories are being used as driving functions.

REFERENCES

1. A. J. Neylan and W. Gorholt, "Design Development of the HTGR Core and Its Support Structure - Seismic Considerations," Nuclear Engineering and Design, 29 (1974), pp. 231-242, North-Holland Publishing Company.

2. John M. Biggs, Introduction to Structural Dynamics (McGraw Hill Book Co, NY, 1964), pp. 30-31.

3. J. L. Merson and J. G. Bennett, "A Computer Method for Analyzing HTGR Core Block Response to Seismic Excitation," Los Alamos Scientific Laboratory report in preparation.

4. Glenn Murphy, Similitude in Engineering, (Ronald Press Co, NY 1950).

5. "SIMEAR" a program developed by M. Watabe, University of California at Berkeley, available through the National Information Service, Earthquake Engineering, Berkeley, CA.

TABLE I

"PROTOTYPE" AND "MODEL" STUDY PARAMETERS

	PROTOTYPE	TRUE MODEL	DISTORTED MODEL	DISTORTED MODEL
d_p =	0.381 m (15 in)	0.381/4 m	0.381/4 m	0.381/4 m
C_p =	0.381 cm (0.15 in)	0.381/4 cm	0.381/4 cm	0.381/4 cm
μ_{s_p} =	0.200	0.200	0.200	0.2 x 4
μ_{k_p} =	0.160	0.160	0.160	0.16 x 4
E_p =	13.79×10^9 N/m^2 (2×10^6 psi)	$\left(\frac{E_m}{W_m} = \frac{E_p}{W_p} \times 4^2\right)$	13.97×10^9 N/m^2	13.97×10^9 N/m^2
W_p =	975.94 N (219.4 lb)		975.94/4^3 N	975.94/4^3 N
X_B =	$\pm$0.9944 cm ($\pm$0.3915 in)	$\pm$0.9944/4 cm	$\pm$0.9944/4 cm	$\pm$0.9944/4 cm
f_B =	5 Hz	$5 \times \sqrt{4} = 10$ Hz	$5 \times 4 = 20$ Hz	$5 \times 4 = 20$ Hz
i.e. =	$\ddot{X}_B$ = 1g	1g	4g	4g
	SCALES:			
	LENGTH - N_d	$\sqrt[4]{4}$	4	4
	TIME - N_T		4	4
	ACCELERATION - $N_{\ddot{x}}$	1	1/4	1/4
	FORCE - N_Q	$E_p/E_m \times 4^2$	4^2	4^2
	STRESS - N_σ	$N_Q \div 4^2$	1	1

TABLE II

BASE VALUES USED IN THE STUDY OF THE TWO-DIMENSIONAL MODEL

Item	Symbol	Base Value
Block Size	d	0.38 m (15 in)
Block Weight	W	794 N (178.5 lb)
Block Stiffness		
Horizontal direction	K_H	1.89×10^9 N/m (10.8×10^6 lb/in)
Vertical direction	K_v	2.84×10^9 N/m (16.2×10^6 lb/in)
Connector Stiffness		
Pin	K_p	1.084×10^9 N/m (6.19×10^6 lb/in)
Slot	K_s	1.084×10^9 N/m (6.19×10^6 lb/in)
Gap Between Block	C	0.38 cm (0.150 in)
Clearance Between Pin and Slot	h	0.127 cm (0.050 in)
Friction Between Horizontal Surfaces		
Static Coefficient	μ_s	0.20
Kinetic Coefficient	μ_k	0.16
Base Motion - Horizontal		
Frequency	f_B	5 Hz
Amplitude	$\ddot{X}_B$	1g
Base Motion - Vertical	Y_B	0

TABLE III

EFFECT OF PIN CLEARANCE AND STIFFNESS

Description[a]	Max Block Acceleration (9)	Max. Side Contact Force (N)	Max. Pin Shear Force (N)
1-D System (block 1,2,3,4 only), no pins	345	274×10^3 (61,677 lb)	-----
2-D System (block 1-16) no pins	377	299×10^3 (67,281 lb)	0
2-D System Base Values	178	131×10^3 (29,520 lb)	140×10^3 (31, 597 lb)
2-D System "h" decreased to 0.0254 cm (0.010 in)	72	0 (no side contact)	57×10^3 (12,879 lb)
2-D System "h" increased to 0.254 cm (0.100 in)	327	260×10^3 (58,344 lb)	169×10^3 (38,006 lb)
2-D System K_p and K_s increased to 1.75×10^9 N/m	219	128×10^3 (28,820 lb)	173×10^3 (38,966 lb)
2-D System K_p and K_s decreased to 0.7×10^9 N/m	164	130×10^3 (29,200 lb)	115×10^3 (25,907 lb)

[a] All values are as given in Table II, except as noted.

NRC-8

INTERNAL DISTRIBUTION

No. of Copies	Name of Recipient
10	R. C. Dove
10	J. G. Bennett
10	J. L. Merson
25	R-4 Group Office
20	WX-8 Group Office
25	W. G. Davey

EXTERNAL DISTRIBUTION

Distribution for NRC-8